Potential mechanism of TMEM2/CD44 in endoplasmic reticulum stress-induced neuronal apoptosis in a rat model of traumatic brain injury

MUYAO WU[1*], CHAOYU WANG[1*], YATING GONG[1], YAQIAN HUANG[1], LEI JIANG[1], MIN ZHANG[2], RONG GAO[3] and BAOQI DANG[1]

Departments of [1]Rehabilitation and [2]Preventive Treatment, Zhangjiagang TCM Hospital Affiliated to Nanjing University of Chinese Medicine; [3]Department of Neurosurgery, The Affiliated Zhangjiagang Hospital of Soochow University, Zhangjiagang, Jiangsu 215600, P.R. China

Received June 19, 2023; Accepted October 6, 2023

DOI: 10.3892/ijmm.2023.5322

Abstract. Traumatic brain injury (TBI) can lead to the disruption of endoplasmic reticulum (ER) homeostasis in neurons and induce ER stress. Transmembrane protein 2 (TMEM2) may regulate ER stress through the p38/ERK signaling pathway, independent of the classic unfolded protein response (UPR) pathway. The present study examined the expression of TMEM2 following TBI in a rat model, in an aim to determine whether the mitogen-activated protein kinase (MAPK) signaling pathway is controlled by TMEM2/CD44 to mitigate secondary brain injury. For this purpose, 89 Sprague-Dawley rats were used to establish the model of TBI, and TMEM2 siRNA was used to silence TMEM2. Western blot analysis, immunofluorescence, TUNEL assay and Fluoro-Jade C staining, the wet-dry method and behavioral scoring were used for analyses. The results revealed that TMEM2 was activated following TBI in rats. The silencing of TMEM2 resulted in a significant increase in the levels of p38 and ERK (components of MAPK signaling), while brain edema, neuronal apoptosis and degeneration were significantly aggravated. TBI increased TMEM2/CD44-aggravated brain edema and neurological impairment, possibly by regulating ERK and p38 signaling. TMEM2/CD44 may thus be a target for the prevention and control of TBI.

Correspondence to: Dr Baoqi Dang, Department of Rehabilitation, Zhangjiagang TCM Hospital Affiliated to Nanjing University of Chinese Medicine, 77 Changan Southern Road, Zhangjiagang, Jiangsu 215600, P.R. China
E-mail: doctor_dang82@hotmail.com

Dr Rong Gao, Department of Neurosurgery, The Affiliated Zhangjiagang Hospital of Soochow University, 68 Jiyang Western Road, Zhangjiagang, Jiangsu 215600, P.R. China
E-mail: 714866001@qq.com

*Contributed equally

Key words: transmembrane protein 2, CD44, traumatic brain injury, endoplasmic reticulum stress, MAPK pathway

Introduction

Traumatic brain injury (TBI) is caused by blunt, penetrating and accelerating or decelerating forces. Symptoms of TBI include decreased levels of consciousness, memory loss or amnesia, and other neurological or neuropsychological abnormalities. TBI, which occurs mostly in young individuals, is one of the major causes of disability, and in some cases, can lead to death (1). Indeed, TBI is the third most common cause of mortality worldwide. The annual global incidence of TBI is >294 per 100,000 individuals (2,3). TBI severely affects the quality of life of affected individuals and is associated with a wide range of disabilities, including sensory, motor and cognitive impairments, as well as affective disorders (4). In addition to primary mechanical injury occurring immediately following trauma, secondary brain injuries, such as delayed intracranial hemorrhage, oxidative stress, local inflammatory response and blood-brain barrier injury, play a major role in neuronal death (1,5). Following brain cell injury, the Ca^{2+} homeostasis of the endoplasmic reticulum (ER) of neurons is destroyed, which can cause ER stress; thus, ER stress is involved in the pathophysiology of TBI (6,7).

The ER is an important cellular organelle responsible for protein modification and processing, as well as the folding, assembly and transportation of new peptide chains (8). The unfolded protein response (UPR) is the classic pathway that regulates the ER stress response. Following the abnormal over-accumulation of proteins in the ER, protein kinase R-like ER kinase (PERK), activating transcription factor 6 (ATF6) and inositol-requiring protein 1 (IRE1) exhibit signs of stress (9). As a result, they signal the nucleus and trigger a cellular response that leads to a decrease in protein synthesis and an increase in ER capacity, initiating the ER stress mechanism (10,11). If the ER stress cannot be resolved through the aforementioned three pathways, the UPR can also maintain the stability of the intracellular environment by affecting cell signals mediated by multiple mitogen-activated protein kinase

(MAPK) signaling pathways, such as extracellular regulated protein kinases (ERKs), p38 MAPK and C-Jun N-terminal kinase (JNK) (12). The UPR is involved in the biosynthetic stress of the ER, and the pathways involved serve to maintain cellular homeostasis. By contrast, stress-activated MAPK pathways are regulated by a diverse array of intracellular and extracellular stresses and regulate cell death and aging by integrating signals from the UPR, other cell stress responses and other cellular signaling pathways (13,14).

In the context of ER stress, a number of pathologies are characterized by changes in the cellular microenvironment, including changes in the composition of hyaluronic acid (HA) in the extracellular matrix (ECM). HA, a key component of the ECM, participates in critical tasks, such as receptor protein attachment and intercellular communication (15,16). In a recent study, transmembrane protein 2 (TMEM2), a cell surface hyaluronidase, was shown to convert high-molecular-weight hyaluronan (HMW-HA) into low-molecular-weight hyaluronan (LMW-HA) to regulate ER stress, and this process was likely mediated via the CD44-p38/ERK signaling pathway (17).

TMEM2 is a recently discovered specific cell surface hyaluronidase, which has been proven to be an effective regulator of ER stress. TMEM2 participates in the regulation of ER stress through the decomposition of HA in the ECM (2). CD44, a cell adhesion molecule, is a transmembrane glycoprotein encoded by a single gene, which is commonly expressed on the surface of various cells and tissues (18,19). CD44 can affect apoptosis by participating in ER stress (20). Recent studies have demonstrated that TMEM2 can decompose HMW-HA (molecular weight >1,000 kDa) into LMW-HA (molecular weight of ~20 kDa). These decomposed HMW-HAs can enter cells through CD44 and affect p38/ERK signal transduction, improve ER stress resistance and protect cells from damage induced by ER stress (17). Notably, TMEM2 has been shown to prolong the lifespan and improve the immunity of nematode worms, and this pathway is independent of the classic UPR pathway after ER stress (17). The present study investigated the association between TMEM2 and neuronal apoptosis following TBI. The authors aimed to clarify the neuroprotective role of TMEM2 in TBI and determine whether it regulates ER stress and inhibits the activation of the p38/ERK signaling pathway through CD44 to alleviate brain edema and nerve cell death.

Materials and methods

Study design and grouping. A rat model TBI of was employed in the present study, and two blind experiments were performed, as illustrated in Fig. 1. The rats exhibited no obvious differences in body weight, feed intake and motor function.

Experiment 1 was conducted to determine the time course of TMEM2 and CD44 post-TBI (Fig. 1B). A total of 36 rats (36 surviving out of an initial cohort of 38) were randomly divided into the sham-operated (sham), TBI 12-h, TBI 1-day, TBI 2-day, TBI 3-day and TBI 7-day groups (6 rats per group). Following the induction of TBI (as described below), the brain tissue surrounding the damaged area was collected and divided (Fig. 1A). Western blot (WB) analysis was performed on the tissues collected from the front of the damaged area, while tissues collected from the rear were subjected to double immunofluorescence analysis.

Experiment 2 was conducted to establish the role of the TMEM2/CD44 signaling pathway in TBI (Fig. 1C). A total of 48 rats (48 surviving out of a group of 51) were randomly assigned to the sham, TBI 2-day, TBI + siRNA TMEM2 and TBI + vehicle groups (12 rats per group). At 2 days post-TBI, which was based on Experiment 1, the animals were euthanized and injured brain tissues were collected. Tissues from 6 rats in each group were assessed using WB analysis, terminal deoxynucleotidyl transferase-mediated dUTP nick-end labeling (TUNEL) staining and Fluoro-Jade C (FJC) staining. An additional 6 rats from each group were evaluated for brain edema, and 6 rats per group were randomly selected for neurological score assessment prior to euthanasia (2% sodium pentobarbital, 150 mg/kg, i.p.) (Fig. 1C).

Animals. A total of 89 male Sprague-Dawley rats (weighing 280-320 g; 8 weeks old) were provided by Zhaoyan New Drug Research Center (Suzhou, China), of which 84 were analyzed as two rats from Experiment 1 and 3 rats from Experiment 2 died (the rats did not recover from breathing arrest during modeling) during anesthesia or modeling. The humane endpoints used in the present study were cyanosis, dyspnea, mental depression and severe hypothermia (<37˚C). The rats were provided food and water *ad libitum*. The rats were kept in an environment with a constant temperature (25˚C) and humidity (50%), with a 12-h light/dark cycle. The experimental protocols were approved by the Animal Ethics and Welfare Committee (AEWC) of Zhangjiagang TCM Hospital Affiliated to Nanjing University of Chinese Medicine (Zhangjiagang, China; protocol code 2022-4-1), and conformed to the guidelines on the care and use of animals outlined by the National Institutes of Health.

Establishment of the rat model of TBI. Experimental TBI was established in the rats, as described in a previous study (21). The rats underwent intraperitoneal anesthesia with 1% sodium pentobarbital at 40 mg/kg and fixation onto a stereotaxic apparatus (Shanghai Yuyan Instruments Co., Ltd.). A 5-mm parietal window to the right of the midline and behind the coronal suture was created with a bone drill, and the dura remained intact. A copper weight (4 mm in diameter and 5 mm in height) was then placed in the bone window, and a 40-g steel rod was dropped from a height of 25 cm onto the copper weight to induce trauma. A short pause in the rat heart rate and breathing indicated successful modeling. Following disinfection and suturing, the rats were allowed to recover in a warm room. The rats in the sham group were subjected to the aforementioned procedure, but without the steel rod step.

TMEM2 siRNA injection. At 24 h prior to the induction of TBI, the TMEM2 siRNA and control siRNA groups received an intracerebroventricular injection (500 pmol; Thermo Fisher, Inc.) after the rats were anesthetized (1% sodium pentobarbital, 40 mg/kg, i.p.), mixed with *in vivo* RNA transfection reagent [Engreen Biosystem Ltd. (China)], according to a previously described method (22). TMEM2 siRNA/control siRNA was added into 2 μl nuclease-free water to 500 pmol, and then mixed with 1 μl transfection reagent, to a total solution of 3 μl. The TMEM2 siRNA was purchased from Thermo Fisher Scientific, Inc. A non-targeted siRNA control (Thermo Fisher

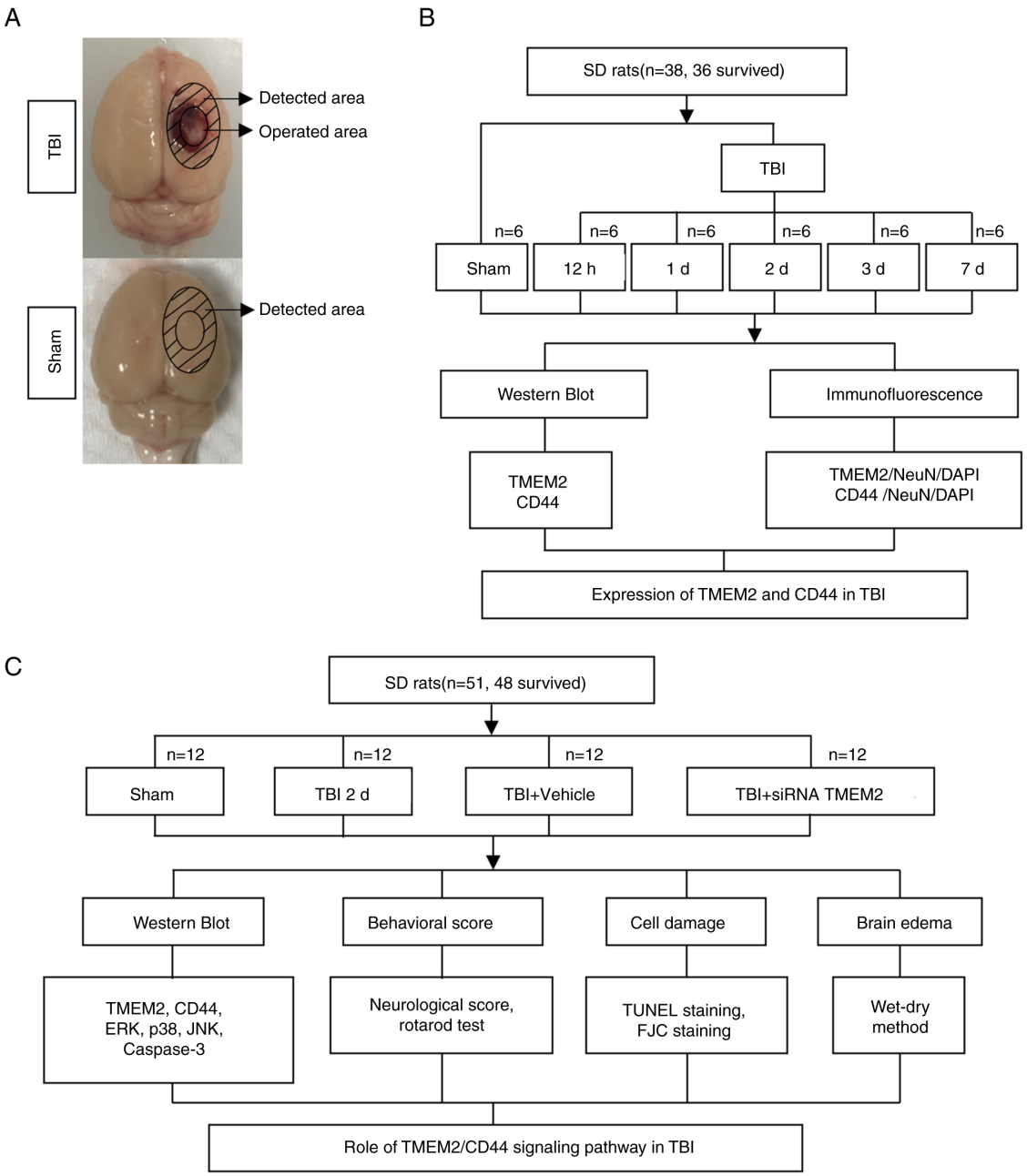

Figure 1. Rat model of TBI and study design. (A) Brain tissues obtained from the TBI group or from the same location in the sham group were assessed. (B) Expression of TMEM2 and CD44, their locations in nerve cells post-TBI, and the determination of the optimal time point for the subsequent experiment. (C) Analysis of the effects of the TMEM2/CD44-MAPK pathway post-TBI and elucidation of the potential mechanisms behind these effects. TBI, traumatic brain injury; TMEM2, transmembrane protein 2; sham, sham-operated; d, days.

Scientific, Inc.) was used as the control siRNA in the TBI + vehicle group.

Tissue collection and sectioning. 1% sodium pentobarbital (40 mg/kg, i.p.) anesthesia was performed at the indicated time points post-injury. The rats were perfused transcardially with 200 ml 0.9% normal saline, and cortical specimens around the injury area (3 mm from the edge of the injury site in the TBI group or the same location in Sham animals) were obtained and placed on ice (Fig. 1A). A portion of the specimens underwent snap freezing and storage at -80˚C for use in WB analysis. The remaining samples were fixed in 4% formalin overnight, embedded in paraffin and sectioned at a thickness of 5 μm with a paraffin slicer (SLEE medical GmbH) for immunofluorescence, TUNEL assay and FJC staining. The tissue samples were extracted and selected by two pathologists who were blinded to the grouping.

WB analysis. WB analysis was conducted using a previously published method (23). Brain tissues were mixed with a tissue protein extraction reagent (CWBio) containing protease inhibitors before being homogenized on ice for 20 min. The homogenates were isolated by centrifugation at 12,000 x g and 4˚C. A Pierce™ BCA Protein Assay kit (Thermo Fisher Scientific, Inc.) was used for protein quantification. Equal amounts of total protein (30 μg) were resolved by SDS-PAGE and electro-transferred onto a

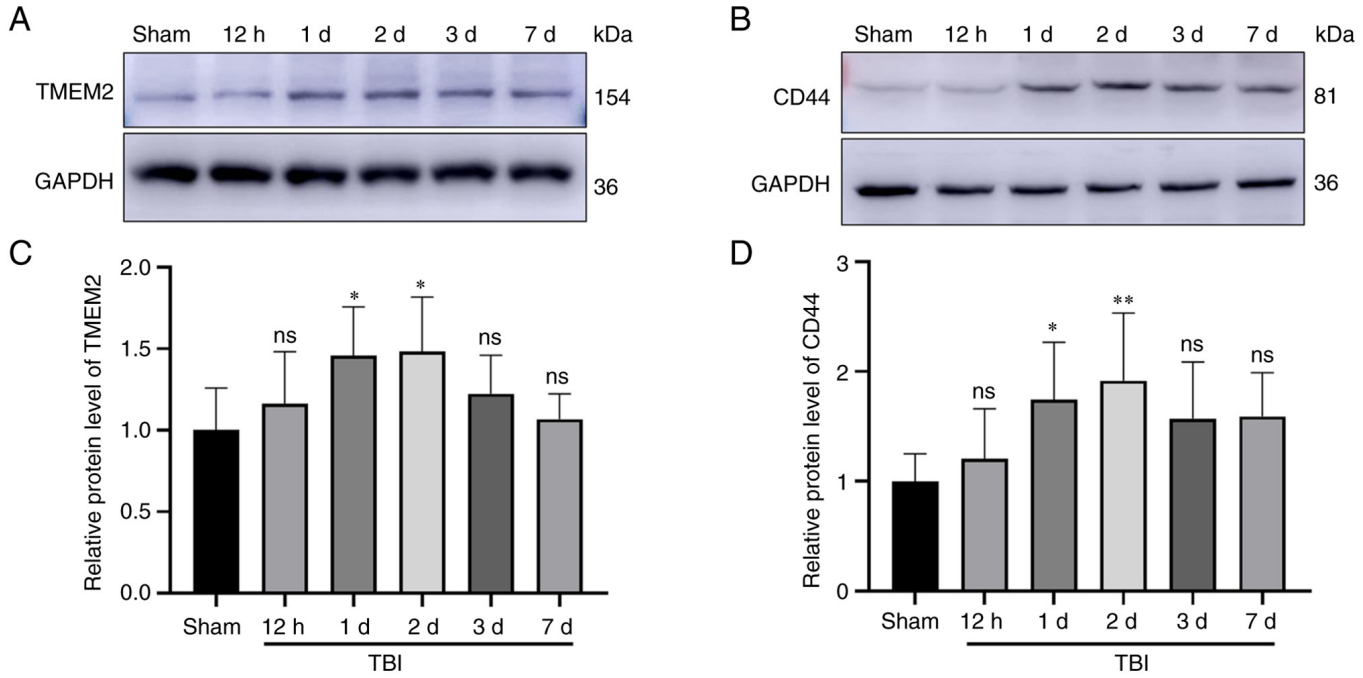

Figure 2. Expression of TMEM2 and CD44 in the injured cortex following TBI. (A and C) TMEM2 and (B and D) CD44 expression levels in the TBI and sham groups at 12 h, and 1, 2, 3 and 7 days, as determined using western blot analysis. The relative densities of each protein were normalized to those of the sham group. Quantification was performed using ImageJ software, and the mean value of the sham group was normalized to 1. Statistical analysis was performed using a one-way analysis of variance (ANOVA), followed by the Dunnett's post-hoc test; n=6 rats in each group. *P<0.05 and **P<0.01, compared to the Sham group; ns, not significant (P>0.05). TBI, traumatic brain injury; TMEM2, transmembrane protein 2; sham, sham-operated; d, days.

PVDF membrane (MilliporeSigma). Following membrane blocking with QuickBlock™ Blocking Buffer (Beyotime Institute of Biotechnology) at an ambient temperature (25˚C) for 1 h, primary antibodies were added followed by incubation overnight at 4˚C. Subsequently, goat anti-rabbit (1:5,000; cat. no. 65-6120, Invitrogen; Thermo Fisher Scientific, Inc.) or anti-mouse IgG-HRP (1:5,000; cat. no. 62-6520, Invitrogen; Thermo Fisher Scientific, Inc.) were added followed by incubation at an ambient temperature (25˚C) for 1 h. Finally, immunoblots were detected using the Immobilon™ Western Chemiluminescent HRP Substrate (Millipore), visualized with an imaging system (Bio-Rad Laboratories, Inc.), and quantified using ImageJ 1.8.0 software (National Institutes of Health). The primary antibodies used in this experiment were as follows: Rabbit anti-TMEM2 (1:1,000; cat. no. ab98348), rabbit anti-CD44 (1:2,000; cat. no. ab157107), rabbit anti-p38 (1:1,000; cat. no. ab31828), rabbit anti-phosphorylated (p-)p38 (1:1,000; cat. no. ab4822), rabbit anti-ERK (1:1,000; cat. no. ab184699), rabbit anti-p-ERK (1:1,000; cat. no. ab201015), rabbit anti-JNK (1:1,000; cat. no. ab179461), rabbit anti-p-JNK (1:2,000; cat. no. ab307802) and rabbit anti-caspase-3 (1:2,000; cat. no. ab184787) (all from Abcam), with rabbit anti-GAPDH (1:1,0000, MilliporeSigma) used as the loading control.

Immunofluorescence staining. Double immunofluorescence staining was conducted as described in a previous study (24). After dewaxing, the paraffin-embedded sections were treated with an immunostaining permeable solution (Beyotime Institute of Biotechnology) to rupture the cell membranes. The cells were washed with phosphate-buffered physiological saline (PBS) three times. Subsequently, the sections were blocked with immunostaining block solution (Beyotime Institute of Biotechnology) at an ambient temperature (25˚C) for 30 min and incubated at 4˚C overnight with the following primary antibodies: Rabbit anti-TMEM2 (1:100, cat. no. ab98348, Abcam), rabbit anti-CD44 (1:100, cat. no. ab157107, Abcam) and mouse anti-NeuN (1:300, cat. no. MAB377, Millipore, Merck). Following incubation, the sections were washed three times with PBS and incubated with the secondary antibodies, Alexa Fluor 488 donkey anti-rabbit IgG antibody (1:800, cat. no. A-21206, Invitrogen; Thermo Fisher Scientific, Inc.) and Alexa Fluor 555 donkey anti-mouse IgG antibody (1:800, cat. no. A32773, Invitrogen; Thermo Fisher Scientific, Inc.), for 1 h at room temperature. Finally, 4',6-diamidino-2-phenylindole dihydrochloride (DAPI) was used for counterstaining at room temperature (25˚C) for 10 min, and the sections were imaged with a fluorescence microscope (Olympus Corporation).

Neurological assessment. Neurological evaluation was performed 2 days post-TBI, as previously described (25). The scoring system consisted of the following seven components: i) Spontaneous activity; ii) axial sensation; iii) vibrissae proprioception; iv) symmetry of limb movement; v) lateral turning; vi) forelimb outstretching; and vii) climbing. Each subtest was scored from 0 to 3, with a maximum score of 21, where higher scores indicated less nerve damage.

Rotarod test. The rats were trained for 3 days prior to TBI by placing them on an accelerated rotation cylinder with multiple runways. After turning on the machine, the speed was slowly increased from 4 to 40 r/min for 5 min, during which time the rats walked on it to prevent falling. The trial ended if the animal fell off the pedal. The duration the rats spent on the device was recorded.

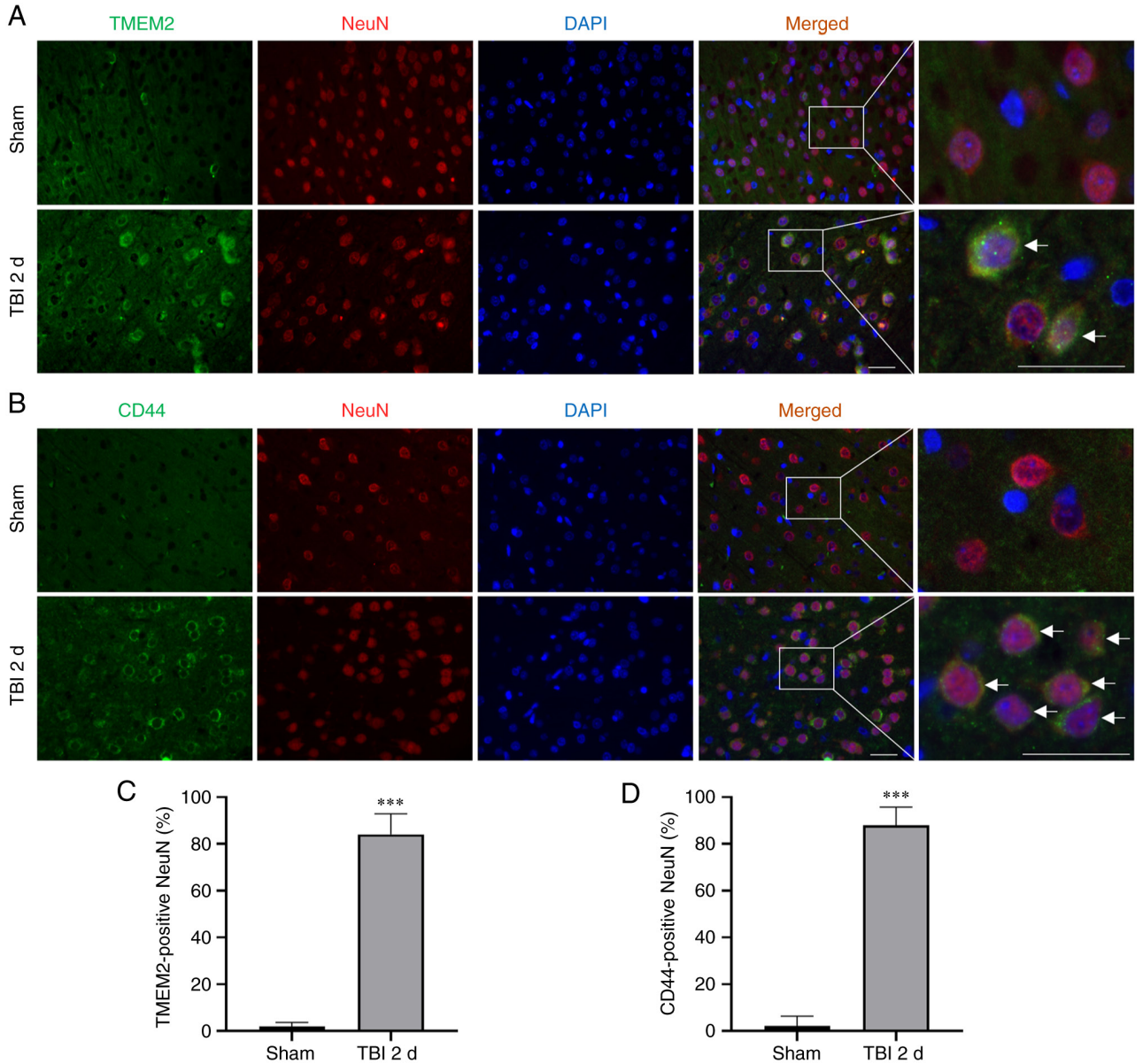

Figure 3. Localization of TMEM2 and CD44 in the injured cortex following TBI. In the sham group and the TBI 2-day group, the expression of green-labeled (A and C) TMEM2 and (B and D) CD44, and red-labeled NeuN was measured using double immunofluorescence. The nuclei were stained with DAPI (blue) fluorescence. Scale bar, 50 mm. Statistical analyses were conducted using a Student's t-test; n=6 rats in each group. ***P<0.001, compared to the sham group. TBI, traumatic brain injury; TMEM2, transmembrane protein 2; sham, sham-operated; d, days.

TUNEL staining. TUNEL assay was conducted to measure apoptosis, as per the manufacturer's instructions (Beyotime Institute of Biotechnology). Following dewaxing in xylene, the paraffin-embedded sections were treated for 20 min with DNase-free proteinase K (20 μg/ml) at 37˚C, followed by a 1-h incubation with TUNEL working solution at 37˚C in the dark. Subsequently, DAPI Fluoromount-G™ [Yeasen Biotechnology (Shanghai) Co., Ltd.] was used for counterstaining at room temperature (25˚C) for 10 min prior to observation under a fluorescent microscope (Olympus Corporation). The apoptotic index was calculated as follows: (TUNEL-positive cells)/(total cells) x100%.

FJC staining. Degeneration was measured using FJC staining, as per the manufacturer's instructions (Biosensis). After dewaxing in xylene, the paraffin-embedded sections were transferred to solution B [potassium permanganate and distilled water (1:9, v/v)] and incubated for 10 min. The sections were then incubated with solution C [FJC solution and distilled water (1:9, v/v)] for 30 min in the dark and washed with distilled water. After drying at 60˚C for 10 min, the specimens were soaked in xylene for 5 min and sealed with a Neutral Balsam [Yeasen Biotechnology (Shanghai) Co., Ltd.] prior to observation under a fluorescent microscope (Olympus Corporation).

Brain edema. The assessment of brain edema was conducted using the wet-dry method, as previously described (26). After separating the rat brains, the brain sections were split into ipsilateral and contralateral sides, and the wet weight was immediately determined with an electronic balance (ME104/02, Mettler Toledo). Next, the brain tissues were dried

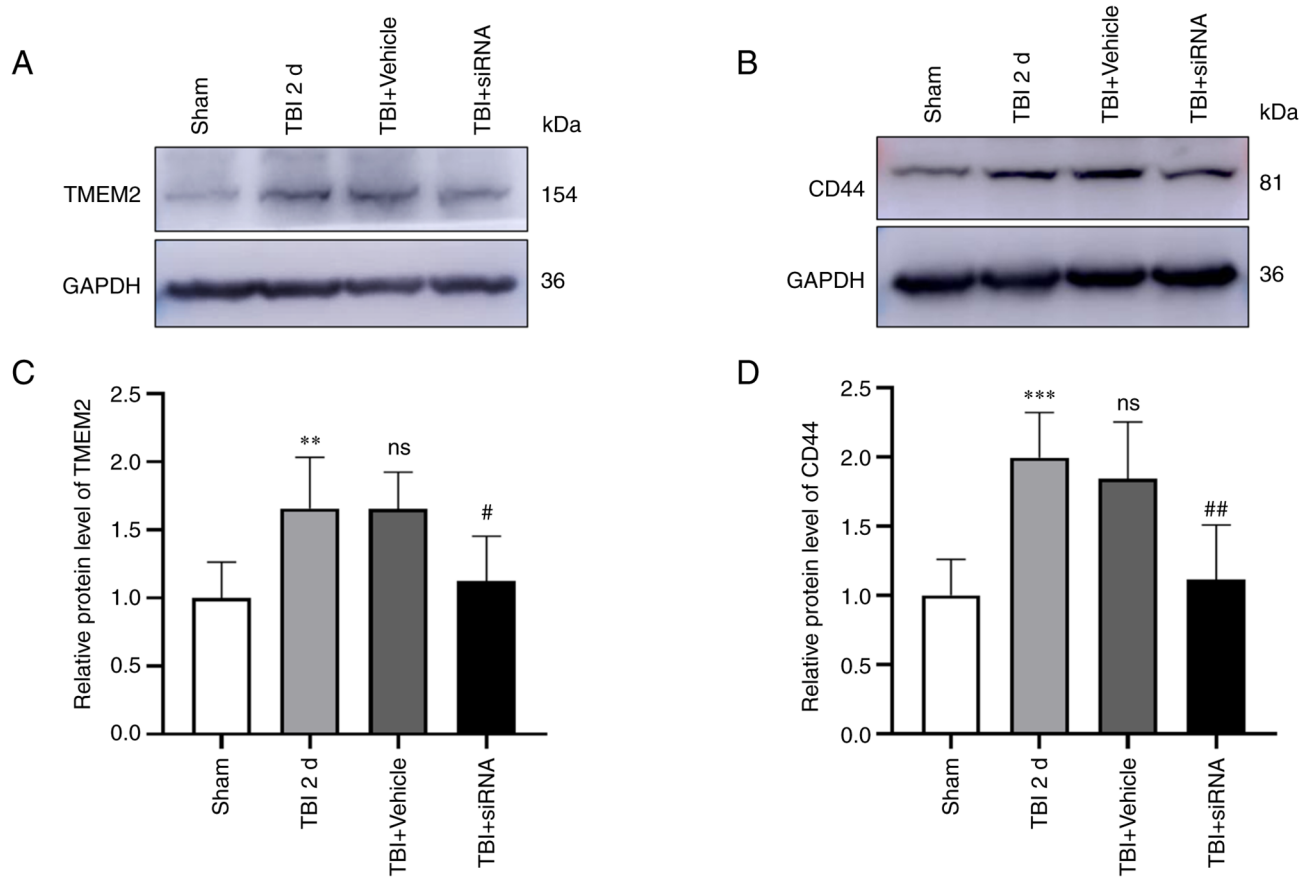

Figure 4. Expression of TMEM2 and CD44 proteins following intervention with TMEM2 siRNA post-TBI. The protein expression levels of (A and C) TMEM2 and (B and D) CD44 were detected using western blot analysis. Statistical analyses were performed using a one-way ANOVA, followed by Tukey's post hoc test; n=6 rats in each group. **P<0.01 and ***P<0.001, compared to the sham group; $^{\#}$P<0.05 and $^{\#\#}$P<0.01, compared to the TBI + vehicle group; ns, not significant (P>0.05), compared to the TBI 2-day group. TBI, traumatic brain injury; TMEM2, transmembrane protein 2; sham, sham-operated; d, days.

at 100˚C for 24 h, and the dry weights were obtained. The brain water content was quantified as follows: [(wet weight-dry weight)/wet weight] x100%.

Statistical analyses. Data are expressed as the mean ± standard deviation, and GraphPad Prism 8.0 (GraphPad Prism, Inc.) was used for analysis. A one-way analysis of variance (ANOVA) with post-hoc Dunnett's multiple test was performed to compare the experimental groups with the Sham group in Fig. 2. A Student's t-test was performed for the analysis of two groups (Fig. 3). A one-way ANOVA with Tukey's multiple comparisons post hoc test was performed to compare multiple groups (Figs. 4-7; apart from Fig. 7E). A two-way ANOVA with Tukey's multiple comparisons post hoc test was conducted to analyze brain edema (Fig. 7E). A value of P<0.05 was considered to indicate a statistically significant difference.

Results

TMEM2 and CD44 protein levels in the rat brain following TBI. The amount of TMEM2 and CD44 proteins was determined at 12 h, and 1, 2, 3 and 7 days post-TBI using WB analysis. The TMEM2 expression levels were elevated at 12 h post-TBI and peaked at 2 days (Fig. 2A and C). The CD44 expression levels were consistent with those of TMEM2 and were increased at 12 h post-TBI, and peaked at 2 days (Fig. 2B and D). Both the TBI 1-day and 2-day groups differed significantly from the sham group.

TMEM2 and CD44 expression in neurons following TBI. Double immunofluorescence staining for NeuN was used to determine the expression of TMEM2 and CD44. At 2 days post-TBI, the number of TMEM2-positive neurons (Fig. 3A and C) and CD44-positive neurons (Fig. 3B and D) increased in the TBI group compared to the sham group.

Effects of TMEM2 siRNA on TMEM2 and CD44 expression following TBI. Compared to the sham group, the expression of TMEM2 (Fig. 4A and C) and CD44 (Fig. 4B and D) increased significantly in the TBI group, and the expression in the TBI and TBI + vehicle groups was comparable. Additionally, the TMEM2 and CD44 expression levels were markedly reduced in the TBI + siRNA group compared to the levels in the TBI + vehicle group.

Effects of TMEM2 siRNA on the MAPK signaling pathway following TBI. Compared to the sham group, the expression of p-p38 (Fig. 5A and B) and p-ERK (Fig. 5C and D) was significantly increased in the TBI group, with comparable amounts in the TBI and TBI + vehicle groups. Additionally, the expression of p-p38 and p-ERK in the TBI + siRNA group

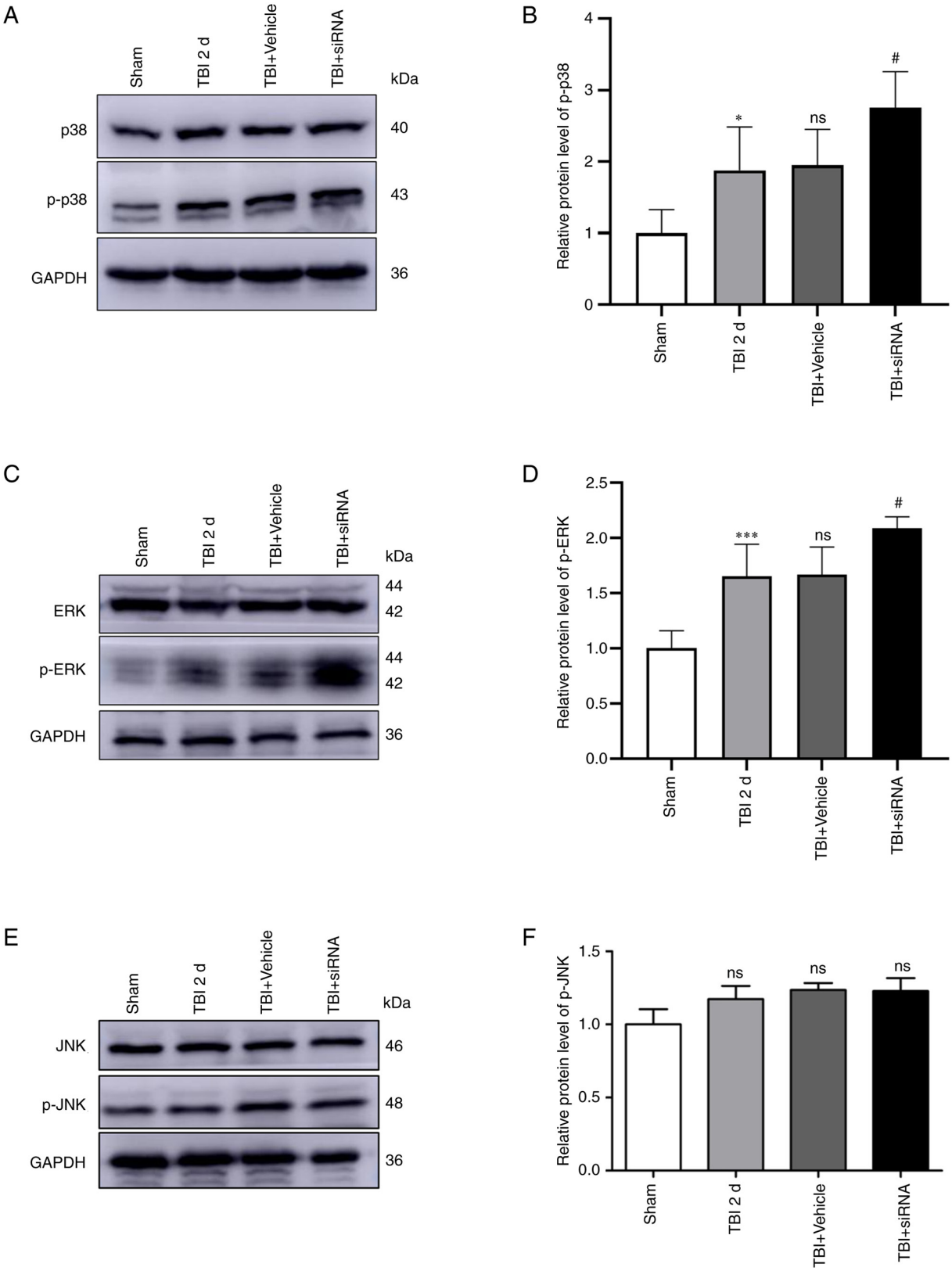

Figure 5. Expression of MAPK signaling following intervention with TMEM2 siRNA post-TBI. Protein expression levels of (A and B) p38/p-p38, (C and D) ERK/p-ERK, and (E and F) JNK/p-JNK at 2 days post-TBI. Statistical analyses were performed using a one-way ANOVA, followed by Tukey's post hoc test; n=6 rats in each group. *P<0.05 and ***P<0.001, compared to the sham group; $^{\#}$P<0.05, compared to the TBI + vehicle group; ns, not significant (P>0.05), compared to the TBI 2 d group. TBI, traumatic brain injury; sham, sham-operated; d, days.

was markedly increased compared to that in the TBI + vehicle group. However, the expression of p-JNK did not differ significantly among the four groups (Fig. 5E and F).

Neuronal apoptosis and degeneration in rats with TBI following intervention with TMEM2 siRNA. The expression of caspase-3 (Fig. 6A and B) was evaluated, and TUNEL staining

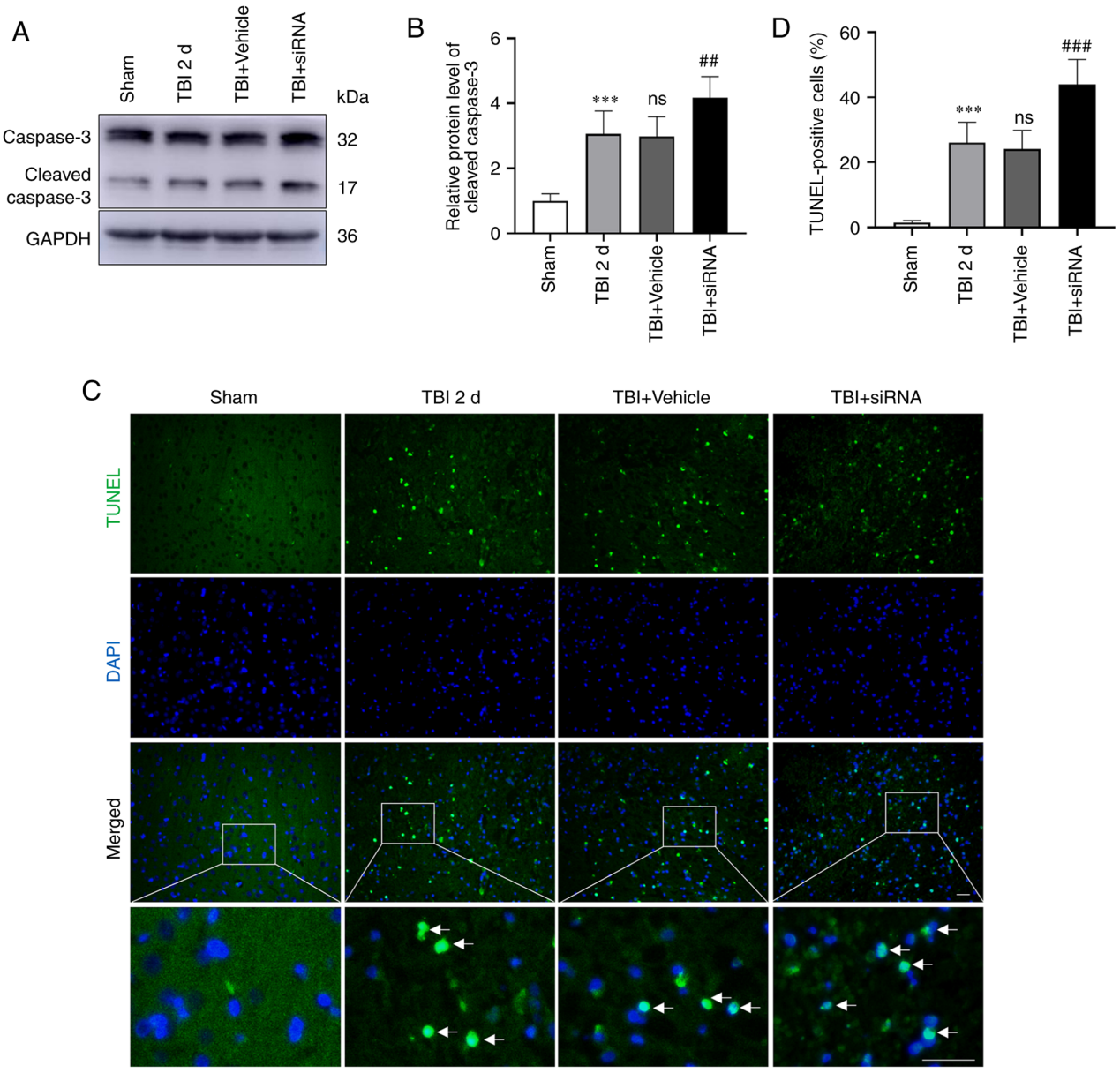

Figure 6. Effects of intervention with transmembrane protein 2 siRNA on apoptosis 2 days post-TBI. Protein expression levels of (A and B) caspase-3 and (C and D) TUNEL staining were used to detect neuronal apoptosis. TUNEL-positive (green) apoptotic cells and DAPI-stained (blue) nuclei are shown. Scale bar, 100 mm. Statistical analysis was conducted using a one-way ANOVA, followed by Tukey's post hoc test; n=6 rats in each group. ***P<0.001, compared to the sham group; $^{\#\#}$P<0.005 and $^{\#\#\#}$P<0.001, compared to the TBI + vehicle group; ns, not significant (P>0.05), compared to the TBI 2-day group. TBI, traumatic brain injury; sham, sham-operated; d, days.

(Fig. 6C and D) was performed to determine the extent of neuronal apoptosis, while FJC staining (Fig. 7A and B) was performed to reflect degeneration. The results revealed that neuronal apoptosis and degeneration were elevated in the TBI and TBI + vehicle groups compared to the sham group. Moreover, the TBI and TBI + vehicle groups had similar rates of neuronal degeneration and apoptosis. Following TMEM2 siRNA intervention, neuronal degeneration and apoptosis increased in the TBI + siRNA group compared to those in the TBI + vehicle group.

Brain edema and behavioral scores following intervention with TMEM2 siRNA. Compared to the sham group, the brain water content in the injured hemispheres was significantly elevated in the TBI group. The TBI and TBI + vehicle groups had comparable brain water content. Additionally, post-TBI, cerebral edema was significantly enhanced following intervention with TMEM2 siRNA (Fig. 7C). Additionally, the neurological score (Fig. 7D) and rotarod test duration (Fig. 7E) were reduced in the TBI groups compared to those in the sham group. Moreover, the scores in the TBI + siRNA group were substantially lower than those in the TBI + vehicle group.

Discussion

TMEM2 is a type II transmembrane protein expressed in numerous organs and systems, including the heart, brain, spinal cord, eyes, heart, lungs, liver, kidneys, spleen, skeletal muscle, articular cartilage, lymph node, bone marrow, thymus, bladder and synovium (27,28). However, the expression

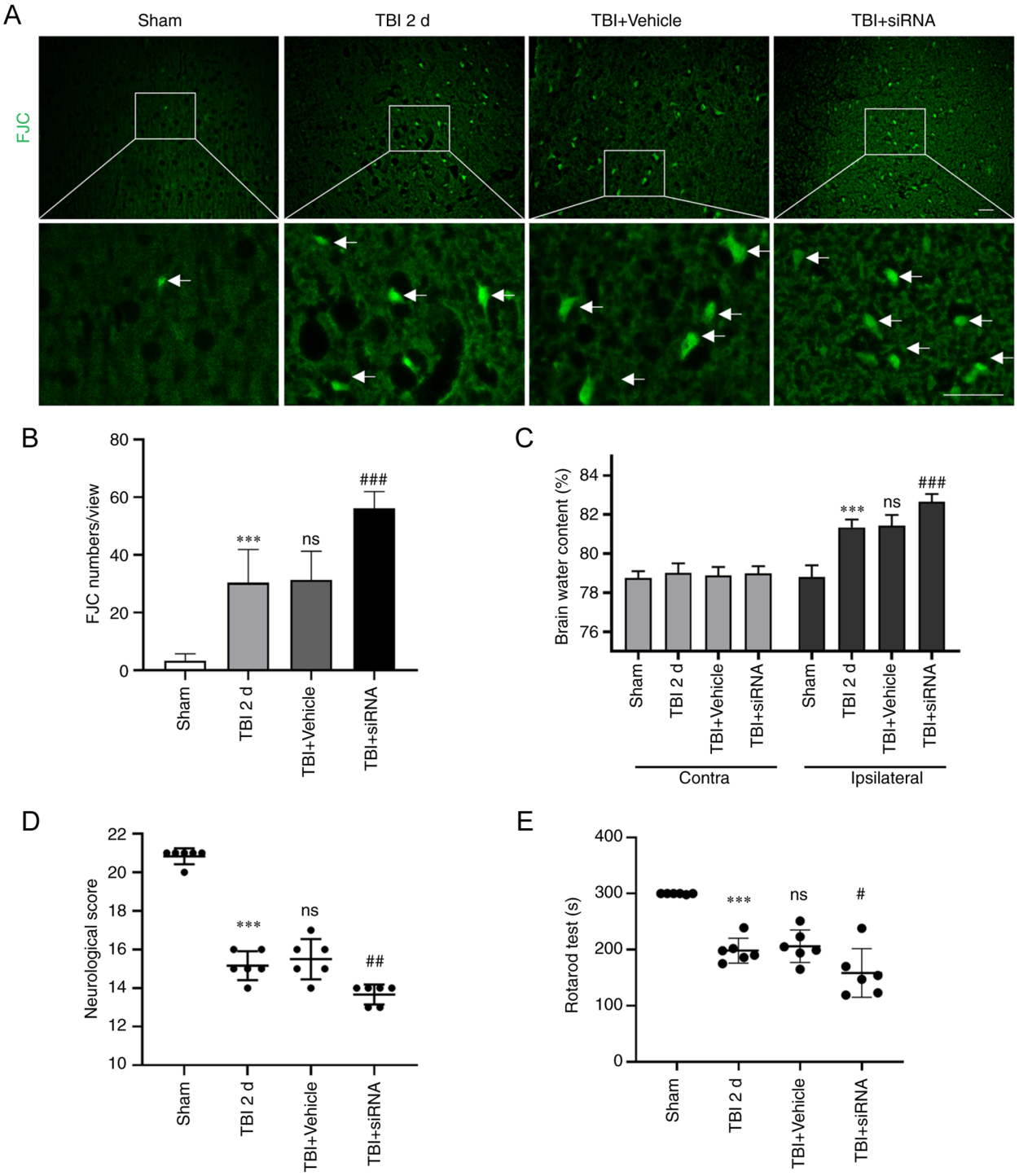

Figure 7. Degeneration, brain edema and behavioral scores following intervention with transmembrane protein 2 siRNA post-TBI. (A and B) FJC (green) staining was performed to detect degeneration. (C) Brain edema was measured using the wet-dry method. (D) Neurological scores and (E) the rotarod test were used to reflect behavioral scores. Statistical analyses were performed using a one-way ANOVA, followed by the Tukey's post-hoc test (except brain edema), and brain edema analysis was performed using a two-way ANOVA followed by the Tukey's post-hoc test; n=6 rats in each group. ***P<0.001, compared to the sham group; $^{\#}$P<0.05, $^{\#\#}$P<0.01 and $^{\#\#\#}$P<0.001, compared to the TBI + vehicle group. ns, not significant (P>0.05), compared to the TBI 2-day group. TBI, traumatic brain injury; sham, sham-operated; d, days.

and function of TMEM2 are limited under various pathophysiological conditions. The present study investigated the neuroprotective effects of TMEM2/CD44 in rats with TBI and the possible underlying mechanisms. Post-TBI, the expression of TMEM2 was increase in the rats and peaked after 2 days (Fig. 2A and C). Double-immunofluorescence staining revealed that TMEM2 was expressed on the surface of neuron cells, as shown in Fig. 3A. Previous studies have demonstrated that TMEM2 is located on the plasma membrane, and represents a newly discovered cell surface HA-degrading enzyme (29). Additionally, TMEM2 has been shown to be involved in maintaining ER homeostasis (17) and to promote angiogenesis (30).

When ER stress is induced by cell injury, the sensors of UPR (PERK, IRE1 and ATF6) are activated to restore ER

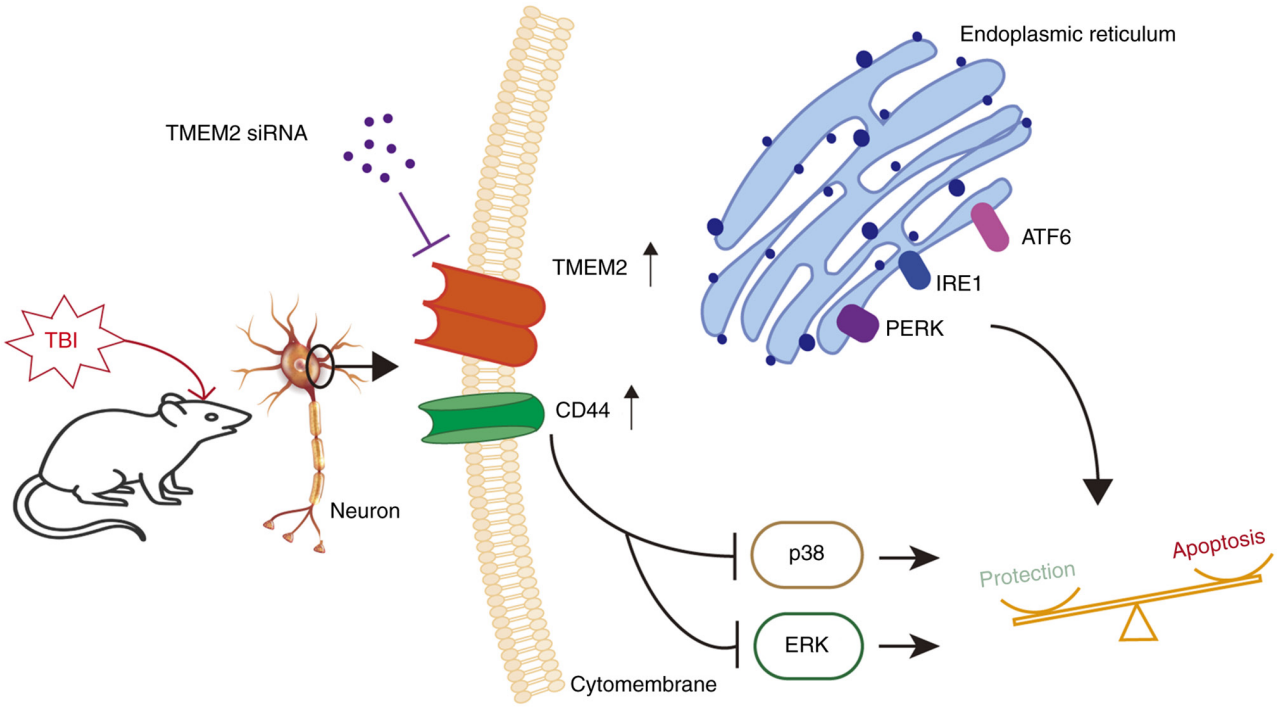

Figure 8. Model illustrating the possible mechanisms underlying the effects of TMEM2 on secondary brain injury after TBI. TMEM2 and CD44 were activated to alleviate the degree of secondary brain injury by inhibiting p38 and ERK signaling of the MAPK pathway following TBI. Silencing TMEM2 may aggravate the degree of secondary brain injury. TBI, traumatic brain injury; TMEM2, transmembrane protein 2; ATF6, activating transcription factor 6; PERK, protein kinase R-like ER kinase; IRE1, inositol-requiring protein 1.

homeostasis by blocking the synthesis of some proteins, as well as by enhancing ER-specific molecular chaperones, protein degradation pathways and autophagy (31). When irreparable damage occurs, the UPR participates in the terminal response, leading to apoptotic clearance (32), which has been reported in the TBI model (33). In addition, the MAPK signaling pathway (including p38, ERK and JNK pathways) is also known to regulate apoptosis following ER stress. If ER stress is not alleviated following injury, it will trigger cell death or aging by influencing the MAPK signaling; this mechanism enables cells to have certain flexibility during ER stress and can regulate cell fate according to internal and external signals (13,34). Attenuating the phosphorylation of p38 and ERK can improve the neurological score following TBI (35). Alleviating ER stress and inhibiting the phosphorylation of MAPK signaling can improve apoptosis (36). TMEM2 responds to ER stress through the MAPK pathway, independent of UPR signals and maintains ER homeostasis. This sequence of events was discovered by Schinzel *et al* (17), who found that TMEM2 overexpression protected wild-type human fibroblasts from ER stress by regulating CD44. It has been proven that TMEM2/p38/ERK improves ER folding capacity or limits the damage in response to ER stress (37). However, to the best of our knowledge, no previous study to date has investigated whether TMEM2 regulates TBI-induced ER stress through the MAPK pathway. In the present study, the expression of TMEM2 was found to increase in the surrounding brain tissue following TBI (Fig. 2A). When TMEM2 was silenced using siRNA, the CD44 expression levels were decreased (Fig. 4B), the expression of p-p38 and p-ERK was increased (Fig. 5A and C) and secondary brain injury following TBI was aggravated (Figs. 6 and 7). These results indicate that TMEM2 exerts a protective effect on rats with TBI through the p38/ERK pathway.

With the activation of the UPR, a number of pathological manifestations in neurodegenerative diseases and some malignant tumors exhibit significant changes in the cellular microenvironment. Changes in the ER stress response and glycosaminoglycan and HA composition in the ECM have been observed (38,39). TMEM2 degrades HA in the ECM in a Ca^{2+}-dependent manner, resulting in HA internalization and complete degradation in the lysosome (29,40). HA is a large macromolecule and one of the main components of the ECM (41). Genetic and chemical inhibition of typical UPR components suggests that HA decomposition increases ER stress resistance. Low-molecular-weight fragments of HA appear to be involved in regulating the MAPK pathway components, p38 and ERK, by activating CD44 receptors and maintaining cell viability under conditions of stress (42). The hyaluronidase activity of TMEM2 and its products provide protection against ER stress and mediate ER stress resistance through the CD44/MAPK pathway. Therefore, the present study investigated the effects of TMEM2 on secondary brain injury in rats with TBI through MAPK signaling. The results revealed that when TMEM2 was silenced using TMEM2 siRNA following TBI, the expression of TMEM2 and CD44 decreased (Fig. 4), and the expression of p-p38 and p-ERK increased (Fig. 5A and C), which aggravated apoptosis (Figs. 5E and 6B) and degeneration (Fig. 5A). However, the silencing of TMEM2 had no effect on the expression of p-JNK (Fig. 5E). Previous research has also found that TMEM2 mediates ER stress through the CD44 and MAPK signaling

pathways (ERK and p38 signaling) and protects cells from ER stress (17). Although the JNK pathway can also mediate apoptosis (43), as also demonstrated in the present study, TMEM2/CD44 did not affect apoptosis through the JNK pathway, and the specific mechanisms remain to be explored.

As a hyaluronidase, TMEM2 can decompose HA by dissolution mechanisms, as well as decompose HA from HMW-HA (>1,000 kDa) to LMW-HA (~20 kDa) (29,30). Specifically, TMEM2 is responsible for degrading the extracellular HMW-HA into moderate-molecular-weight HA (MMW-HA, 200-1,000 kDa). The intracellular lysosomal hyaluronidase and glucosidase further process the MMW-HA into smaller fragments (27). HA is involved in numerous processes, including receptor protein attachment and intercellular communications (44). HMW-HA exerts anti-inflammatory and anti-angiogenic effects, while LMW-HA promotes inflammatory and angiogenic responses (45,46). However, it does exert a neuroprotective effect on the nervous system (47,48).

The present study had certain limitations, which should be mentioned. The present study did not investigate the changes and effects of HA following TBI. Moreover, it was not verified whether TMEM2 decomposes HMW-HA into LMW-HA, or whether LMW-HA enters cells to play a neuroprotective role. Therefore, in future studies, the authors aim to verify the effects of HA on secondary brain injury following TBI *in vivo* and *in vitro*. Previous studies have also shown that HA regulates cell adhesion, migration and proliferation through various interactions with specific receptors on cell surfaces, such as CD44 (44,45). However, the possibility of the interaction between HA and CD44 was did not explore herein; therefore, the authors aim to evaluate the association between HA and CD44 on the cell surface by co-immunoprecipitation in future studies.

In conclusion, the present study investigated the role of TMEM2 in a rat model of TBI. The results revealed that TMEM2 was activated and activated CD44 on the surface of neurons, which induced brain edema and apoptosis by inhibiting the p38 and ERK pathways of MAPK, and alleviated the degree of secondary brain injury (Fig. 8). Moreover, when TMEM2 was silenced, cerebral edema and nerve injury were aggravated by the upregulation of ERK and p38 signals. Therefore, TMEM2/CD44 represents a potential therapeutic target for TBI prevention and control.

Acknowledgements

Not applicable.

Funding

The present study was supported by the Enterprise School Cooperative Education Project of the Ministry of Education (grant no. 202102242005), the Zhangjiagang Key Health Personnel Training Program (grant no. ZJGWSRC202003), the Suzhou Youth Science and Technology Project (grant nos. KJXW2020062 and KJXW2021063), the Suzhou Science and Technology Development Project (grant nos. SKJY2021001 and SKJY2021003), the Suzhou Livelihood Science and Technology Project (grant no. SYS2020054) and the Gusu Health Personnel Training Project (grant no. GSWS2020104).

Availability of data and materials

The datasets used and/or analyzed during the current study are available from the corresponding author upon reasonable request.

Authors' contributions

MW, RG and BD contributed to the conception or design of the study. MW, CW, YG, YH, LJ and MZ contributed to the acquisition of data. MW and CW drafted the manuscript; YG and RG processed the graphs and performed data analysis. MW and BD revised the manuscript. All authors have read and approved the final manuscript. YG, RG and BD confirm the authenticity of all the raw data.

Ethics approval and consent to participate

The present study was conducted in accordance with the Declaration of Helsinki and was approved by the Animal Ethics and Welfare Committee (AEWC) of Zhangjiagang TCM Hospital Affiliated with Nanjing University of Chinese Medicine (protocol code 2022-4-1).

Patient consent for publication

Not applicable.

Competing interests

The authors declare that they have no competing interests.

References

1. Dang B, Chen W, He W and Chen G: Rehabilitation treatment and progress of traumatic brain injury dysfunction. Neural Plast 2017: 1582182, 2017.
2. Nguyen R, Fiest KM, McChesney J, Kwon CS, Jette N, Frolkis AD, Atta C, Mah S, Dhaliwal H, Reid A, *et al*: The International incidence of traumatic brain injury: A systematic review and Meta-Analysis. Can J Neurol Sci 43: 774-785, 2016.
3. Dehghanian F, Soltani Z and Khaksari M: Can mesenchymal stem cells act multipotential in traumatic brain injury? J Mol Neurosci 70: 677-688, 2020.
4. Eastman CL, D'Ambrosio R and Ganesh T: Modulating neuroinflammation and oxidative stress to prevent epilepsy and improve outcomes after traumatic brain injury. Neuropharmacology 172: 107907, 2020.
5. Li D, Ni H, Rui Q, Gao R and Chen G: Deletion of Mst1 attenuates neuronal loss and improves neurological impairment in a rat model of traumatic brain injury. Brain Res 1688: 15-21, 2018.
6. Wu J, He J, Tian X, Zhong J, Li H and Sun X: Activation of the hedgehog pathway promotes recovery of neurological function after traumatic brain injury by protecting the neurovascular unit. Transl Stroke Res 11: 720-733, 2020.
7. Ni H, Rui Q, Xu Y, Zhu J, Gao F, Dang B, Li D, Gao R and Chen G: RACK1 upregulation induces neuroprotection by activating the IRE1-XBP1 signaling pathway following traumatic brain injury in rats. Exp Neurol 304: 102-113, 2018.
8. Oakes SA and Papa FR: The role of endoplasmic reticulum stress in human pathology. Annu Rev Pathol 10: 173-194, 2015.
9. Wang M, Law ME, Castellano RK and Law BK: The unfolded protein response as a target for anticancer therapeutics. Crit Rev Oncol Hematol 127: 66-79, 2018.
10. Choi SI, Lee E, Jeong JB, Akuzum B, Maeng YS, Kim TI and Kim EK: 4-Phenylbutyric acid reduces mutant-TGFBIp levels and ER stress through activation of ERAD pathway in corneal fibroblasts of granular corneal dystrophy type 2. Biochem Biophys Res Commun 477: 841-846, 2016.

11. Katayama T, Imaizumi K, Honda A, Yoneda T, Kudo T, Takeda M, Mori K, Rozmahel R, Fraser P, George-Hyslop PS and Tohyama M: Disturbed activation of endoplasmic reticulum stress transducers by familial Alzheimer's disease-linked presenilin-1 mutations. J Biol Chem 276: 43446-43454, 2001.
12. Liu Y, Guyton KZ, Gorospe M, Xu Q, Lee JC and Holbrook NJ: Differential activation of ERK, JNK/SAPK and P38/CSBP/RK map kinase family members during the cellular response to arsenite. Free Radic Biol Med 21: 771-781, 1996.
13. Hotamisligil GS and Davis RJ: Cell signaling and stress responses. Cold Spring Harb Perspect Biol 8: a006072, 2016.
14. Li W, Zhu J, Dou J, She H, Tao K, Xu H, Yang Q and Mao Z: Phosphorylation of LAMP2A by p38 MAPK couples ER stress to chaperone-mediated autophagy. Nat Commun 8: 1763, 2017.
15. Vasvani S, Kulkarni P and Rawtani D: Hyaluronic acid: A review on its biology, aspects of drug delivery, route of administrations and a special emphasis on its approved marketed products and recent clinical studies. Int J Biol Macromol 151: 1012-1029, 2020.
16. Garantziotis S and Savani RC: Hyaluronan biology: A complex balancing act of structure, function, location and context. Matrix Biol 78-79: 1-10, 2019.
17. Schinzel RT, Higuchi-Sanabria R, Shalem O, Moehle EA, Webster BM, Joe L, Bar-Ziv R, Frankino PA, Durieux J, Pender C, *et al*: The hyaluronidase, TMEM2, promotes ER homeostasis and longevity independent of the UPR(ER). Cell 179: 1306-1318.e18, 2019.
18. He X, Shi X, Puthiyakunnon S, Zhang L, Zeng Q, Li Y, Boddu S, Qiu J, Lai Z, Ma C, *et al*: CD44-mediated monocyte transmigration across Cryptococcus neoformans-infected brain microvascular endothelial cells is enhanced by HIV-1 gp41-I90 ectodomain. J Biomed Sci 23: 28, 2016.
19. Thorne RF, Legg JW and Isacke CM: The role of the CD44 transmembrane and cytoplasmic domains in co-ordinating adhesive and signalling events. J Cell Sci 117: 373-380, 2004.
20. Dalal S, Zha Q, Daniels CR, Steagall RJ, Joyner WL, Gadeau AP, Singh M and Singh K: Osteopontin stimulates apoptosis in adult cardiac myocytes via the involvement of CD44 receptors, mitochondrial death pathway, and endoplasmic reticulum stress. Am J Physiol Heart Circ Physiol 306: H1182-H1191, 2014.
21. Gao F, Li D, Rui Q, Ni H, Liu H, Jiang F, Tao L, Gao R and Dang B: Annexin A7 levels increase in rats with traumatic brain injury and promote secondary brain injury. Front Neurosci 12: 357, 2018.
22. Shi M, Gong Y, Wu M, Gu H, Yu J, Gao F, Ren Z, Qian M, Dang B and Chen G: Downregulation of TREM2/NF-κB signaling may damage the blood-brain barrier and aggravate neuronal apoptosis in experimental rats with surgically injured brain. Brain Res Bull 183: 116-126, 2022.
23. Gong Y, Wu M, Shen J, Tang J, Li J, Xu J, Dang B and Chen G: Inhibition of the NKCC1/NF-κB signaling pathway decreases inflammation and improves brain edema and nerve cell apoptosis in an SBI rat model. Front Mol Neurosci 14: 641993, 2021.
24. Wu MY, Gao F, Tang JF, Shen JC, Gao R, Dang BQ and Chen G: Possible mechanisms of the PERK pathway on neuronal apoptosis in a rat model of surgical brain injury. Am J Transl Res 13: 732-742, 2021.
25. Feng D, Wang B, Wang L, Abraham N, Tao K, Huang L, Shi W, Dong Y and Qu Y: Pre-ischemia melatonin treatment alleviated acute neuronal injury after ischemic stroke by inhibiting endoplasmic reticulum stress-dependent autophagy via PERK and IRE1 signalings. J Pineal Res: 62, 2017 doi: 10.1111/jpi.12395.
26. Gong Y, Wu M, Gao F, Shi M, Gu H, Gao R, Dang BQ and Chen G: Inhibition of the pSPAK/pNKCC1 signaling pathway protects the bloodbrain barrier and reduces neuronal apoptosis in a rat model of surgical brain injury. Mol Med Rep 24: 717, 2021.
27. Yamaguchi Y, Yamamoto H, Tobisawa Y and Irie F: TMEM2: A missing link in hyaluronan catabolism identified? Matrix Biol 78-79: 139-146, 2019.
28. Scott DA, Drury S, Sundstrom RA, Bishop J, Swiderski RE, Carmi R, Ramesh A, Elbedour K, Srikumari Srisailapathy CR, Keats BJ, *et al*: Refining the DFNB7-DFNB11 deafness locus using intragenic polymorphisms in a novel gene, TMEM2. Gene 246: 265-274, 2000.
29. Yamamoto H, Tobisawa Y, Inubushi T, Irie F, Ohyama C and Yamaguchi Y: A mammalian homolog of the zebrafish transmembrane protein 2 (TMEM2) is the long-sought-after cell-surface hyaluronidase. J Biol Chem 292: 7304-7313, 2017.
30. De Angelis JE, Lagendijk AK, Chen H, Tromp A, Bower NI, Tunny KA, Brooks AJ, Bakkers J, FrancoisM, Yap AS, *et al*: Tmem2 regulates embryonic vegf signaling by controlling hyaluronic acid turnover. Dev Cell 40: 421, 2017.
31. Hetz C: The unfolded protein response: Controlling cell fate decisions under ER stress and beyond. Nat Rev Mol Cell Biol 13: 89-102, 2012.
32. Korennykh A and Walter P: Structural basis of the unfolded protein response. Annu Rev Cell Dev Biol 28: 251-277, 2012.
33. Sun G, Zhao Z, Lang J, Sun B and Zhao Q: Nrf2 loss of function exacerbates endoplasmic reticulum stress-induced apoptosis in TBI mice. Neurosci Lett 770: 136400, 2022.
34. Darling NJ and Cook SJ: The role of MAPK signalling pathways in the response to endoplasmic reticulum stress. Biochim Biophys Acta 1843: 2150-2163, 2014.
35. Zhang J, Yi T, Cheng S and Zhang S: Glucagon-like peptide-1 receptor agonist Exendin-4 improves neurological outcomes by attenuating TBI- induced inflammatory responses and MAPK activation in rats. Int Immunopharmacology 86: 106715, 2020.
36. Chen J, Chen J, Cheng Y, Fu Y, Zhao H, Tang M, Zhao H, Lin N, Shi X, Lei Y, *et al*: Mesenchymal stem cell-derived exosomes protect beta cells against hypoxia-induced apoptosis via miR-21 by alleviating ER stress and inhibiting p38 MAPK phosphorylation. Stem Cell Res Ther 11: 97, 2020.
37. Goncalves RLS and Hotamisligil GS: TMEM2 modulates ER stress in a Non-canonical manner. Cell Metab 30: 999-1001, 2019.
38. Brown MK and Naidoo N: The endoplasmic reticulum stress response in aging and age-related diseases. Front Physiol 3: 263, 2012.
39. Chanmee T, Ontong P and Itano N: Hyaluronan: A modulator of the tumor microenvironment. Cancer Lett 375: 20-30, 2016.
40. Tammi MI, Oikari S, Pasonen-Seppanen S, Rilla K, Auvinen P and Tammi RH: Activated hyaluronan metabolism in the tumor matrix-Causes and consequences. Matrix Biol 78-79: 147-164, 2019.
41. Kudo Y, Sato N, Adachi Y, Amaike T, Koga A, Kohi S, Noguchi H, Nakayama T and Hirata K: Overexpression of transmembrane protein 2 (TMEM2), a novel hyaluronidase, predicts poor prognosis in pancreatic ductal adenocarcinoma. Pancreatology 20: 1479-1485, 2020.
42. Mascaro M, Pibuel MA, Lompardia SL, Diaz M, Zotta E, Bianconi MI, Lago N, Otero S, Jankilevich G, Alvarez E and Hajos SE: Low molecular weight hyaluronan induces migration of human choriocarcinoma JEG-3 cells mediated by RHAMM as well as by PI3K and MAPK pathways. Histochem Cell Biol 148: 173-187, 2017.
43. Bai G, Wang H and Cui N: mTOR pathway mediates endoplasmic reticulum stress-induced CD4+ T cell apoptosis in septic mice. Apoptosis 27: 740-750, 2022.
44. Laurent TC, Laurent UB and Fraser JR: The structure and function of hyaluronan: An overview. Immunol Cell Biol 74: A1-A7, 1996.
45. West DC, Hampson IN, Arnold F and Kumar S: Angiogenesis induced by degradation products of hyaluronic acid. Science 228: 1324-1326, 1985.
46. Vigetti D, Karousou E, Viola M, Deleonibus S, De Luca G and Passi A: Hyaluronan: Biosynthesis and signaling. Biochim Biophys Acta 1840: 2452-2459, 2014.
47. Wang J, Wang X, Wei J and Wang M: Hyaluronan tetrasaccharide exerts neuroprotective effect and promotes functional recovery after acute spinal cord injury in rats. Neurochem Res 40: 98-108, 2015.
48. Wakao N, Imagama S, Zhang H, Tauchi R, Muramoto A, Natori T, Takeshita S, Ishiguro N, Matsuyama Y and Kadomatsu K: Hyaluronan oligosaccharides promote functional recovery after spinal cord injury in rats. Neurosci Lett 488: 299-304, 2011.